

Preparation and photocatalytic activity of hydroxyapatite supported BiOCl nanocomposite for oxytetracycline removal

Pankaj Raizda*, Sourav Gautam, Bhanu Priya, Pardeep Singh

School of Chemistry, Faculty of Basic Science, Shoolini University, Solan 173212, Himachal Pradesh, India

*Corresponding author. E-mail: pankajchem1@gmail.com

Received: 11 February 2015, Revised: 26 November 2015 and Accepted: 25 January 2016

ABSTRACT

The study investigates photocatalytic activity of hydroxyapatite supported BiOCl (BiOCl/HA) in the presence of H₂O₂. BiOCl/HA was prepared by simple hydrolysis method. BiOCl/HA was characterized using scanning electron microscopy (SEM), tunneling electron microscopy (TEM), X-ray diffraction (XRD), energy diffraction X-ray (EDX), Fourier transform infrared spectroscopy (FTIR) and UV-visible (UV-vis) analysis. SEM results confirmed the dispersion of BiOCl onto hydroxyapatite. BiOCl/HA exhibited irregular pleats-like structure having average size of 80 nm. The band gap of BiOCl/HA was found to be 3.42 eV. The solar light was used as radiation source during photocatalysis. Both H₂O₂ and BiOCl/HA had synergistic effect on oxytetracycline removal. The simultaneous adsorption and photocatalysis (A+P) was most efficient process for OTC removal. The photocatalytic degradation of oxytetracycline obeyed pseudo first order kinetics. The effect of process parameters catalyst loading, H₂O₂ concentration, pH and OTC concentration was investigated on photocatalysis. The oxidative removal occurred through hydroxyl radical formation. BiOCl exhibited significant recycle efficiency due to easier separation and stability in reaction solution. Solar/H₂O₂/BiOCl/HA displayed excellent photocatalytic property for degradation of OTC from aqueous solution. Copyright © 2016 VBRI Press.

Keywords: Hydroxyapatite supported BiOCl; H₂O₂; solar light; photocatalysis; oxytetracycline removal.

Introduction

Antibiotics have been considered as emerging pollutants due to their continuous input and persistence in the aquatic ecosystem [1-2]. The annual global usage of antibiotics has been estimated to be 200000 tons [3]. Among all the used antibiotics, oxytetracycline (OTC) is one of the most frequently detected tetracycline in water bodies [4-6]. Due to antibiotic nature, hydrophilic property and stable naphthalene ring structure, OTC release in water bodies has been considered as a threat to aquatic environment [7].

Currently, advanced oxidation processes (AOPs) have emerged as efficient technique for contaminant-removal from wastewater [8]. Among AOPs, semiconductor-mediated photocatalysis has been given great credit because of its potential to destroy wide range of organic pollutants at ambient reaction conditions [9]. During last decade, bismuth oxyhalides have gained attention because of their excellent photo catalytic properties [10]. Huang *et al.* prepared BiOCl, BiO and BiOI based indirect band gap photocatalysts with layered structure [11]. Zhang *et al.* synthesized magnetic Fe₃O₄/BiOCl composite with high visible activity for dye degradation [12]. In previous studies, smaller size of nano-catalysts exhibited higher photocatalytic activity due to increased surface area. However, small particle size of nano-catalysts caused difficult recovery of catalyst from aqueous medium.

Therefore, nano-catalysts need to be immobilized on organic/inorganic materials for improved recycling efficiency. Adsorption of pollutant onto catalyst surface is highly needed for efficient photodegradation process [13-15]. Hydroxyapatite Ca₁₀(PO₄)₆(OH)₂, abbreviated as HA, has great importance in materials chemistry [16]. It has shown excellent adsorption ability for the separation of biomolecules, pollutants and heavy metal ions from aqueous phase [17, 18].

H₂O₂ is used as a homogenous oxidizing agent to degrade pollutants present in wastewater [19]. The use of H₂O₂ becomes more effective when it acts in conjunction with other reagents or energy sources capable of dissociating it to generate OH[•] radicals [19, 20]. The target pollutants are attacked by hydroxyl radicals to degrade organic compounds. The photochemical processes become more effective when coupled with photocatalytic processes [20].

This work was focused on the applicability of BiOCl/HA as photocatalyst for degradation of oxytetracycline. BiOCl/HA was characterized using scanning electron microscopy (SEM), transmission electron microscopy (TEM), X-ray diffraction (XRD), energy dispersive X-ray analysis (EDX), Fourier transform infrared (FTIR) and ultraviolet-visible (UV-Vis) spectroscopy. The synergistic effect between BiOCl/HA and H₂O₂ was also explored for OTC removal. The effect

of various reaction parameters was also evaluated on photodegradation of antibiotic OTC.

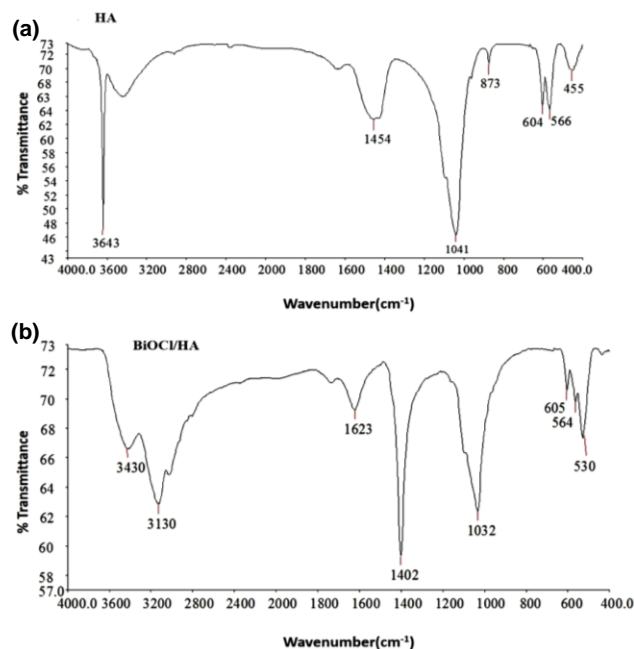


Fig. 1 (a - b). FTIR Spectrum of HA (Hydroxyapatite) (a) and BiOCl/HA (b).

Experimental

Materials and methods

All chemicals used in this study were of analytical grade. Oxytetracycline, tricalcium phosphate $\text{Ca}_3(\text{PO}_4)_2$, bismuth oxide Bi_2O_3 , hydrochloric acid, ammonia and ethanol were purchased from Sigma Aldrich, India and used without further purification. Hen eggshell was collected from local market at Solan, Himachal Pradesh, India. Double distilled water was used to prepare all the solutions.

Preparation of BiOCl/HA

Preparation of CaO from hen eggshell waste

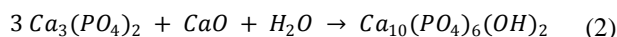
The hen egg shell was washed several time with distilled water and boiled for 2 h [21]. The boiled egg shell waste was heated in muffle furnace at 800 °C for 2 h to obtain CaO powder (Eq. 1).



The obtained CaO was crushed into very fine powdered particles.

Preparation of hydroxyapatite (HA)

In order to prepare HA, 1g of $\text{Ca}_3(\text{PO}_4)_2$ was dissolved in 100 ml of distilled water. To this solution, 1g of prepared CaO was added and continuously stirred for 2 hr (Eq. 2). The obtained mixture was filtered. The precipitates were heated at 200 °C to obtain hydroxyapatite [22].



Preparation of BiOCl/HA

BiOCl/HA was prepared by modified hydrolysis method using bismuth oxide, HCl and HA as precursors [23]. In typical preparation Bi_2O_3 (1.0g) was dissolved in excessive concentrated hydrochloric acid (8.0 mol/L, 8 mL) to obtain a transparent $\text{BiO}_3\text{-HCl}$ aqueous solution. To this solution, 1g of HA was added with simultaneous stirring. The obtained mixture was sonicated for 10 min. The pH of solution was adjusted between 2 and 3 using ammonia. The mixture was heated at 100 °C for half an hour to obtain white precipitates. The precipitates were washed several times with water and ethanol and then dried at 70 °C for 6h to obtain BiOCl/HA.

Photocatalytic experiment

The photocatalytic, photolytic and adsorption experiments were performed in a double walled pyrex vessel (ht. 7.5 cm x dia.6 cm) surrounded by thermostatic water circulation arrangement (30 ± 0.3 °C). During equilibration experiments, slurry composed of H_2O_2 , OTC and catalyst suspension was continuously stirred. The suspension composed of H_2O_2 , OTC and BiOCl/HA was kept under solar light with continuous stirring. At specific time intervals, aliquot (3 mL) was withdrawn and centrifuged for 2 minutes to remove catalyst particles form aliquot. The absorbance of OTC was in supernatant liquid was measured 260 nm. The solar light intensity was measured by digital lux-meter ($35 \times 10^3 \pm 1000$ lx). Photocatalytic experiments were conducted between March to May 2014(11 am to 2 pm). All the experiments were undertaken in triplicate with errors below 5 % and average values were reported. The removal efficiency was calculated using Eq. 3:

$$\% \text{ removal efficiency} = \frac{C_0 - C_t}{C_0} \quad (3)$$

where, C_0 is the initial concentration and C_t is instant concentration of sample.

The kinetics of OTC degradation was described by pseudo first order kinetics. The rate constant (k) and half-life period ($t_{1/2}$) were calculated using Eq. 4 and 5, respectively:

$$k = 2.303 \times \text{slope} \quad (4)$$

$$t_{1/2} = \frac{0.693}{k} \quad (5)$$

where, slope was obtained from the plot of $\ln(c)$ versus t .

Results and discussion

Characterization of HA and BiOCl/HA

FTIR analysis

Fig. 1 displays FTIR spectra of HA and BiOCl/HA. In Fig. 1a, stretching mode of -OH was obtained at 3643 cm^{-1} [24]. The peaks at 1041 cm^{-1} was due to asymmetrical P-O stretching mode of HA [25]. The symmetrical stretching mode of PO_4^{3-} ions was observed at 873 cm^{-1} [26]. The peaks at 604 cm^{-1} and 566 cm^{-1} were ascribed due to P-O bending mode [25]. In BiOCl/HA, peaks at 3430 cm^{-1} and 3130 cm^{-1} were assigned to O-H stretching due to adsorbed H_2O . The peak at 1623.6 cm^{-1} was due to adsorbed atmospheric CO_2 . The characteristic peak of HA at

1041 cm^{-1} was shifted to 1032 cm^{-1} . While other peaks for PO_4^{3-} were observed at 1032.62, 605.70 and 564.6 cm^{-1} . The peak at 530 cm^{-1} was assigned to Bi-O stretching mode [27].

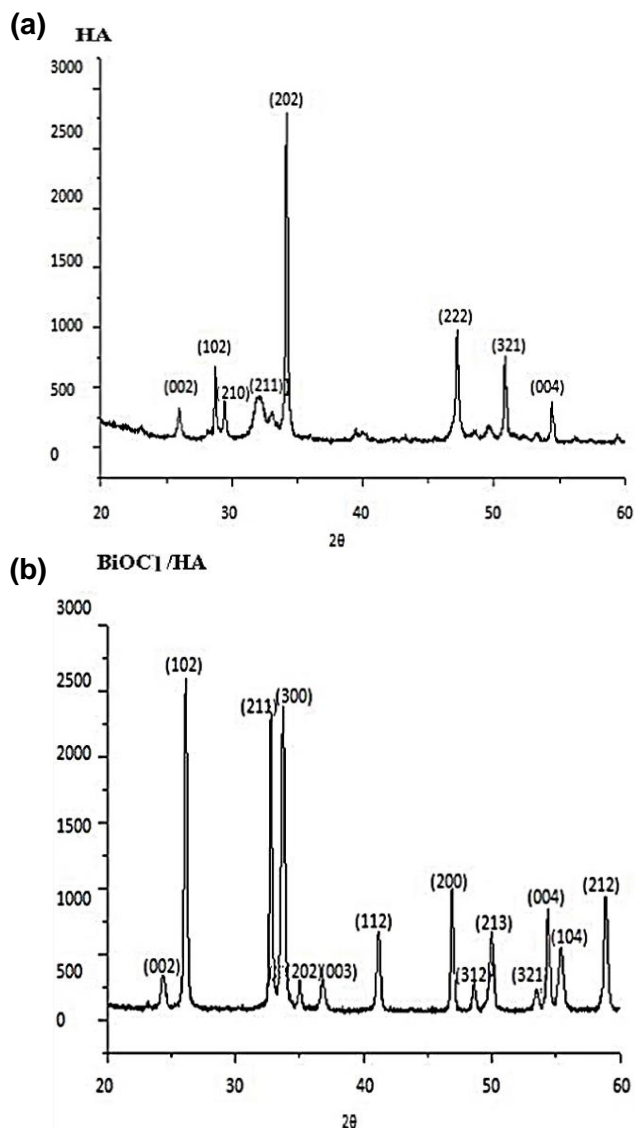


Fig.2 (a - b). XRD pattern of HA (a) and BiOCl/HA(b).

XRD analysis

XRD diffractogram for hydroxyapatite (HA) is shown in **Fig. 2(a)**. Diffraction peaks at 25.93° , 28.60° , 29.43° , 31.95° , 34.19° , 47.07° , 50.84° and 54.34° corresponded to (002), (102), (210), (211), (202), (222), (321), and (004) planes which were in good agreement with the standard JCPDS file (JCPDS# 9-432) for HA. XRD spectrum of BiOCl/HA is shown in **Fig. 2(b)**. Diffraction peaks at 24.33° , 26.17° , 32.78° , 33.67° , 35.02° , 36.70° , 41.18° , 46.88° , 48.56° , 49.91° , 53.49° , 54.38° , 55.28° and 58.28° were due to (002), (102), (211), (300), (202), (003), (112), (200), (312), (213), (321), (004), (104) and (212) planes. XRD pattern indicated semi-crystalline structure of BiOCl/HA. The average size was calculated using Debye Scherer equation and found to be 80 nm.

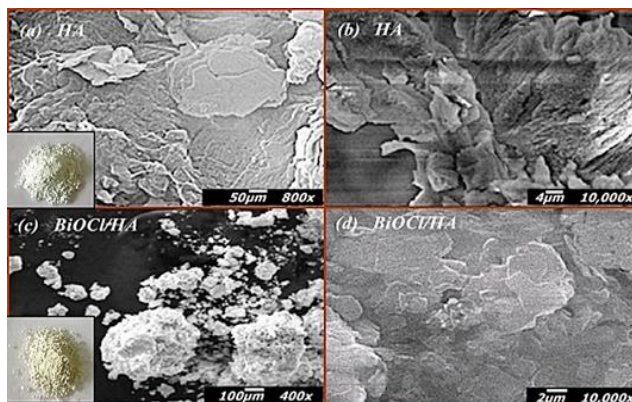


Fig. 3 (a-d). SEM images of HA (a) and BiOCl/HA (b) at different magnifications.

SEM analysis

Fig. 3(a, b) depicts SEM images of HA. HA consisted of agglomerates with irregular shape and porous nature [21]. **Fig. 3(c, d)** displays surface morphology of BiOCl/HA at different magnification. BiOCl particles were unevenly distributed over HA surface.

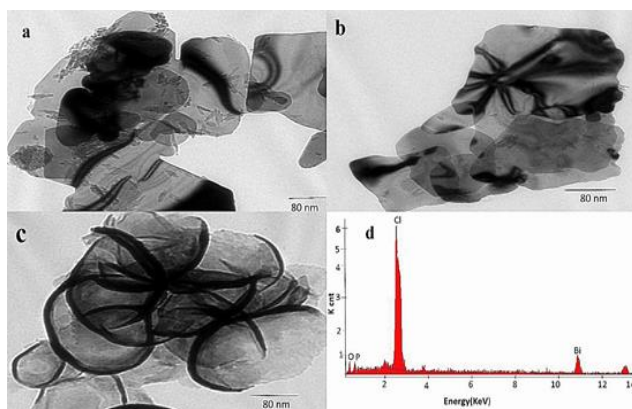


Fig. 4(a-d). TEM images (a-c) and EDX pattern of BiOCl/HA.

TEM and EDX analysis of BiOCl/HA

TEM images of BiOCl/HA are shown in **Fig. 4(a-c)**. BiOCl/HA consisted of irregular pleats-like architecture. The average size of BiOCl/HA was found to be 80 nm which was in good agreement with XRD results. The dark regions in the given images indicated the attachment of BiOCl onto HA surface. **Fig. 4(d)** depicts EDX pattern of BiOCl/HA. The presence of elements O, P, Cl and Bi in BiOCl/HA confirmed the formation of BiOCl/HA.

Optical properties and band gap analysis

Fig. 5 displays UV-vis absorption of BiOCl/HA dispersed in ethanol. The absorption maxima of BiOCl/HA and BiOCl was located at 364 nm and 358, respectively. The band gap of BiOCl/HA was calculated using Tauc relation [28]

$$\alpha h\nu = B(h\nu - E_g)^n \quad (6)$$

where, α = absorption coefficient = $2.303 A/L$, E_g = optical band gap, B = band tailing parameter, $h\nu$ is the photon energy and $n = \frac{1}{2}$ for direct band gap. The band gap was determined by extrapolating straight portion of curve between $(\alpha h\nu)^2$ and $h\nu$ when $\alpha = 0$. The band gap was found to be 3.42 eV.

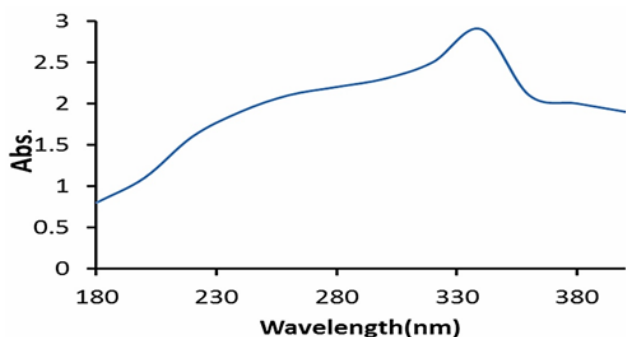


Fig. 5. UV-visible spectrum of BiOCl/HA.

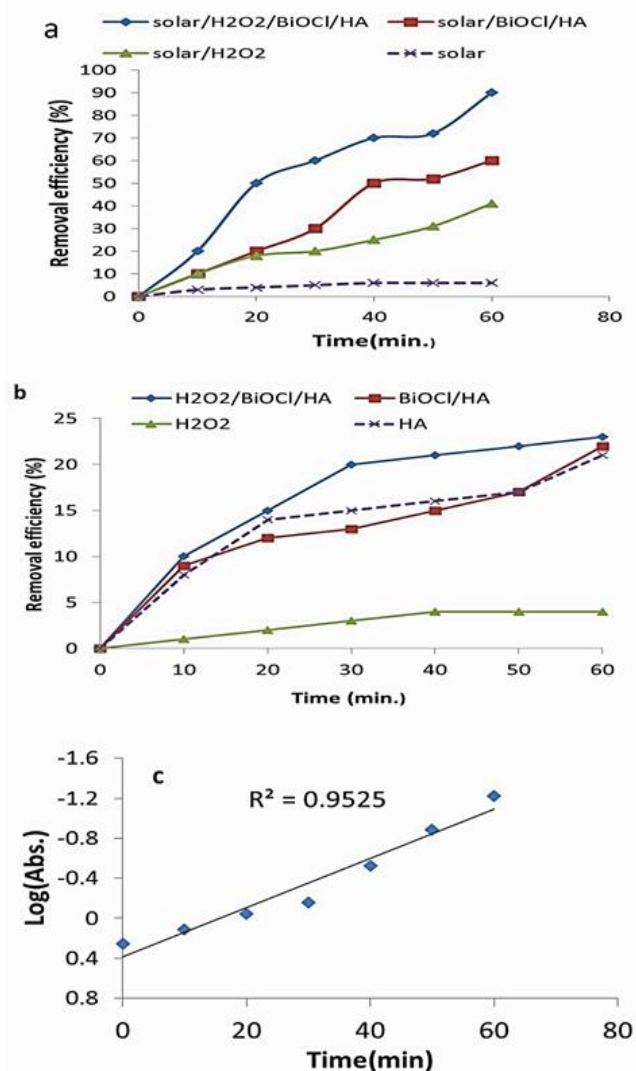


Fig. 6. (a-c). Time profile of OTC degradation under H_2O_2 /BiOCl/HA system under different reaction conditions (a) solar, (b) dark and (c) log (absorbance) v/s time plot. Experimental conditions: $[OTC] = 1 \times 10^{-3} \text{ mol dm}^{-3}$, $[H_2O_2] = 1 \times 10^{-3} \text{ mol dm}^{-3}$, catalyst dosage =

60 mg/50 ml, pH = 5, temperature = $30 \pm 0.3 \text{ }^\circ\text{C}$ and solar light intensity = $35 \times 10^3 \pm 1000 \text{ lx}$.

Oxytetracycline removal under different reaction conditions

In order to compare removal efficiency of different catalytic systems, removal of OTC was investigated under solar/ H_2O_2 /BiOCl/HA, solar/ H_2O_2 solar/BiOCl/HA, and solar treatment systems (Fig. 6 (a)). In solar/ H_2O_2 /BiOCl system, 90 % of OTC was removed in 60 min. While 57 % of OTC was removed using solar/BiOCl catalytic system. In the absence of both H_2O_2 and BiOCl, removal efficiency was negligible. Sequence of OTC removal followed the trend: solar/ H_2O_2 /BiOCl/HA > solar/BiOCl/HA > solar/ H_2O_2 > solar. The experiments were also performed in dark (Fig. 6(b)). The OTC removal followed the trend: H_2O_2 /BiOCl/HA \approx BiOCl/HA \approx HA > H_2O_2 . The higher removal efficiency in case of H_2O_2 /BiOCl/HA, BiOCl/HA and HA system might be due adsorption capacity of HA. However, removal in dark was very low as compared to solar light. In case of solar/ H_2O_2 /BiOCl/HA, the plot for log absorbance versus time followed pseudo first order kinetics with correlation co-efficient of 0.96, rate constant of $5.5 \times 10^{-2} \text{ min}^{-1}$ and half life time of 12.6 min (Fig. 6 (c)).

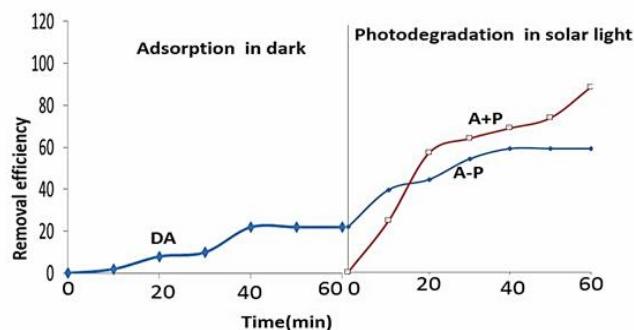


Fig. 7. Real photodegradation process for OTC degradation under solar/ H_2O_2 /BiOCl/HA: Experimental condition: $[OTC] = 1 \times 10^{-3} \text{ mol dm}^{-3}$, $[H_2O_2] = 1 \times 10^{-3} \text{ mol dm}^{-3}$, catalyst dosage = 60 mg/50 ml, pH = 5, temperature = $30 \pm 0.3 \text{ }^\circ\text{C}$ and solar light intensity = $35 \times 10^3 \pm 1000 \text{ lx}$.

Influence of adsorption on photo removal of oxytetracycline

The effect of adsorption on photodegradation was investigated and presented Fig. 7. OTC removal was subjected to three reaction conditions under solar/ H_2O_2 /BiOCl/HA. The three reaction conditions were equilibrium adsorption in dark (DA), equilibrium adsorption followed by photodegradation (A-P) and simultaneous adsorption and degradation (A+P) (Fig. 7). During simultaneous adsorption and degradation process (A+P), 90 % of OTC was degraded under solar light in 60 minute while in case of dark adsorption (DA) only 22 % of OTC was removed (Fig. 7). While during A-P, only 60 % OTC was removed in 120 min. It can visualized that adsorption had positive effect on photodegradation of OTC during A+P. However, in case of A-P, excessive adsorption during first 60 minute deactivated surface of BiOCl/HA leading to lower removal efficiency.

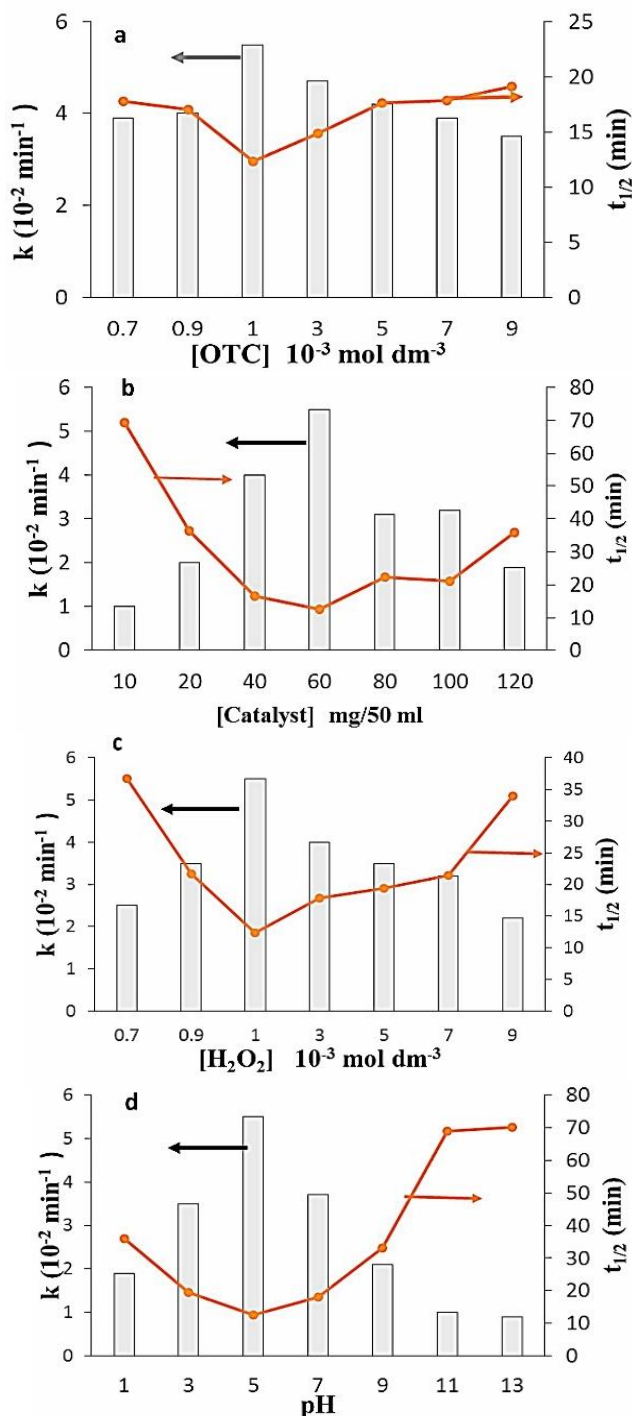


Fig.8 (a-d). Effect of reaction parameter on OTC degradation under solar/ $\text{H}_2\text{O}_2/\text{BiOCl}/\text{HA}$ system. Reaction conditions: $[\text{OTC}] = 1 \times 10^{-3} \text{ mol dm}^{-3}$, $[\text{BiOCl}/\text{HA}] = 60 \text{ mg}/50 \text{ ml}$, $[\text{H}_2\text{O}_2] = 1 \times 10^{-3} \text{ mol dm}^{-3}$, $\text{pH} = 5$, reaction time = 60 min and solar light intensity = $35 \times 10^3 \pm 1000 \text{ lx}$.

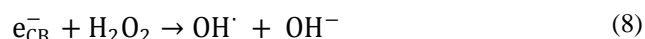
Reaction parameters affecting OTC removal under solar/ $\text{H}_2\text{O}_2/\text{BiOCl}/\text{HA}$ system

OTC degradation rate relates to probability of OH^\cdot radicals formation on catalyst surface and its reaction with OTC. Further, these two factors were influenced by reaction parameters OTC concentration, catalyst loading, pH and H_2O_2 concentration. The effect of reaction parameters was investigated and results are presented in **Fig. 8(a)**. The rate constant increased from $3.9 \times 10^{-2} \text{ min}^{-1}$ to $5.0 \times 10^{-2} \text{ min}^{-1}$

with increase in OTC concentration from $0.7 \times 10^{-4} \text{ M}$ to $5.0 \times 10^{-4} \text{ M}$. Further increase in OTC concentration resulted in decrease in rate constant. The decrease was attributed to the fact that OTC itself started acting as filter for incident radiation and reduced photoactive volume [29, 20].

Under chosen reaction conditions, rate constant increased from $1.0 \times 10^{-2} \text{ min}^{-1}$ to $5.5 \times 10^{-2} \text{ min}^{-1}$ with increase in BiOCl/HA loading from 10 mg/50 ml to 60 mg/50 ml (**Fig.8 (b)**). Thereafter, further increase in catalyst loading resulted in decrease in rate constant. This trend can be rationalized in terms of availability of active sites on BiOCl/HA surface and the penetration of visible light into suspension thus causing an increase in the number of OH^\cdot radical which can take part in actual degradation of OTC. All these factors suggest that optimum amount of BiOCl/HA needs to be added in order to avoid unnecessary excess of catalyst [29, 20].

The effect of H_2O_2 concentration on OTC degradation was studied and results are presented in **Fig.8 (c)**. The rate constant increased rapidly from $2.5 \times 10^{-2} \text{ min}^{-1}$ to $5.5 \times 10^{-2} \text{ min}^{-1}$ on addition of H_2O_2 from $0.7 \times 10^{-3} \text{ mol dm}^{-3}$ to $1 \times 10^{-3} \text{ mol dm}^{-3}$. The added H_2O_2 inhibited electron-hole recombination by accepting photogenerated electron from the conduction band of semiconductor and promotes charge separation and also it forms OH^\cdot radicals according to Eq. (7) and Eq. (8) [29, 30, 20].



Beyond optimal concentration, rate constant decreased with increase in H_2O_2 concentration. When H_2O_2 was in excess it became a scavenger for valence band holes and HO_2^\cdot radical which was a much weaker oxidant than OH^\cdot [20].

The effect of pH on OTC degradation is shown in **Fig 8 (d)**. The rate constant increased from $1.9 \times 10^{-2} \text{ min}^{-1}$ to $5.5 \times 10^{-2} \text{ min}^{-1}$ with increase in pH from 1 to 5. At pH 2, OTC was fully protonated as H_3OTC^+ [1]. At low pH, surface of catalyst was positively charged. It caused lower adsorption of OTC onto catalyst surface. However, majority of OTC changed to zwitter ionic form (H_2OTC^\pm) at pH 5.5 [1]. It resulted in higher adsorption of OTC onto the surface of BiOCl/HA leading to increased rate of OTC degradation. At pH 8.5 and 11, OTC mainly existed as HOTC^- and OTC^{2-} [31, 32]. Above pH 7, negatively charged surface of BiOCl/HA caused poor adsorption of HOTC^- and OTC^{2-} . These factors are responsible for optimal rate constant with half-life period of 12.6 min at pH 5.

Mechanistic view of OTC removal under solar/ $\text{H}_2\text{O}_2/\text{BiOCl}/\text{H}_2\text{O}_2$

In order to explore the role of OH^\cdot radical, OTC removal experiments were performed with isopropanol. Isopropanol containing α -hydrogen is highly reactive with OH^\cdot and poorly with O_2 species. Buxton and co-worker had reported high second order rate constant ($6 \times 10^9 \text{ M}^{-1} \text{ s}^{-1}$) for isopropanol with OH^\cdot radicals [33]. The effect of isopropanol ($2 \times 10^{-4} \text{ mol dm}^{-3}$) on OTC degradation was investigated. The rate of OTC removal was significantly

reduced in the presence of isopropanol. Only 8 % of OTC was removed in the presence of isopropanol due to quenching of OH^\cdot . These results indicated that degradation mainly occurred through OH^\cdot radical assisted oxidative pathway.

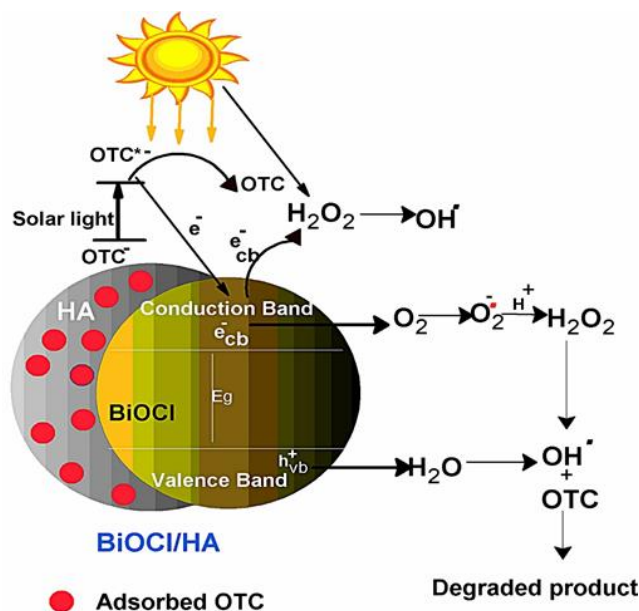
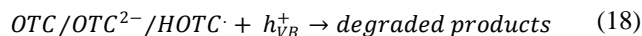
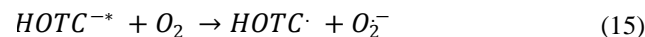
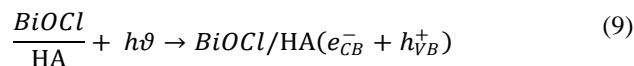


Fig. 9. Mechanistic view of OTC removal using solar/ H_2O_2 /BiOCl/HA.

During photocatalytic process, BiOCl/HA produced conduction band electrons (e_{cb}^-) and valence band holes (h_{vb}^+) (Eq. 9-18). OH^\cdot and ($\text{O}_2^\cdot-$) were also generated directly during illumination of BiOCl/HA catalytic system [34]. H_2O_2 acted as electron scavenger for valence band holes and caused reduction in electron-hole pair recombination. Photo-oxidation and adsorption occur on or near particle surface. At $\text{pH} \approx 5$, HOTC^- was excited to singlet state which crossed to triplet state HOTC^* via intersystem crossing mechanism [1]. The triplet state HOTC^* resulted in injection of electron in conduction band to generate superoxide anion radical ($\text{O}_2^\cdot-$) [1]. HOTC^- also acted as electron scavenger for conduction band electrons. HOTC^* also acted as a sensitizer during solar photocatalytic removal of OTC [1]. The activated $\text{O}_2^\cdot-$ generated H_2O_2 which underwent further reaction responsible for degradation of OTC (Eq. 8). Produced active species leads to oxidative degradation of OTC [35, 36, 7]. Overall mechanism can be explained by (Eq. 9-18) (Fig. 9).



Recycling efficiency is one of most important factor for efficient photocatalytic process. The recycling efficiency of BiOCl/HA catalytic system was explored under solar/ H_2O_2 /BiOCl/HA system. During each run, catalyst was separated from solution through simple sedimentation. The efficiency of BiOCl/HA system was reduced to 74 % from 90% during six cycles. The study showed that BiOCl/HA catalytic system could be easily recycled after six cycles with significant photocatalytic activity (Fig. 10).

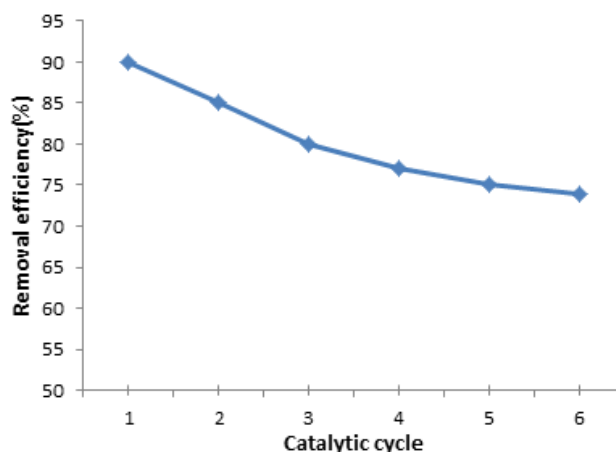


Fig. 10. Recycling efficiency of ZnWO_4/CaO . Reaction conditions: $[\text{OTC}] = 1 \times 10^{-3} \text{ M}$, catalyst dosage = 60 mg/50 ml, $\text{pH} = 5$ and temperature = $30 \pm 1^\circ \text{ C}$, reaction time = 60 min and solar light intensity = $35 \times 10^3 \pm 1000 \text{ lx}$.

Conclusion

Solar photocatalytic degradation thereby proved to be economically cheaper and simpler method for the removal of OTC from aqueous phase. BiOCl/HA catalytic system were successfully synthesized by hydrolysis method. The photocatalytic efficiency of BiOCl/HA nanocomposites was evaluated for the degradation of OTC. Simultaneous adsorption and catalysis process was highly efficient for OTC removal. The degradation of OTC is optimal at $\text{pH} 5$. The rate of reaction was maximal at 60 mg/50 ml of BiOCl/HA loading and $1.0 \times 10^{-3} \text{ M}$ of OTC concentration. The rate constant had maximal value at optimal concentration of H_2O_2 ($1 \times 10^{-3} \text{ mol dm}^{-3}$). The combination of H_2O_2 and BiOCl/HA under solar light was found to be efficient for the degradation of OTC.

Reference

- C. Zhao, M. Pelaez, X. Duan, H. Deng, K. O'Shea, D.F. Kassinos, D.D. Dionysiou, *Appl. Catal. B.*, **2013**, 83-92,134. DOI:10.1016/j.apcatb.2013.01.003.
- B. Halling-Sorensen, S. Nors-Nielsen, P.F. Lanzky, F. Ingerslev, H.C. Holten Lutzhoft, S.E. Jorgensen, *Chemosphere.*, **1998**, 36,2,357. DOI:10.1016/S0045-6535(97)00354-8
- K. Kümmerer, *Chemother*, **2003**, 52, 1, 5. DOI:10.1093/jac/dkg293

4. A.K. Sarmah, M.T. Meyer, A. Boxall, *Chemosphere.*, **2006**, 65,5, 725.
DOI: [10.1016/j.chemosphere.2006.03.026](https://doi.org/10.1016/j.chemosphere.2006.03.026)
5. A.J. Watkinson, E.J. Murby, D.W. Kolpin, S.D. Costanzo, *Sci. Total Environ.* **2009.**, 407, 8, 2711.
DOI: [10.1016/j.scitotenv.2008.11.059](https://doi.org/10.1016/j.scitotenv.2008.11.059)
6. T.A. Ternes, M. Meisenheimer, D. McDowell, F. Sacher, H.J. Brauch, B. Haist-Gulde, N. Zulei-Seibert, *Environ. Sci. Technol.*, **2002.**, 36,17, 3855.
DOI: [10.1021/es015757k](https://doi.org/10.1021/es015757k)
7. A. Kumar, I. Xagorarakis, *Sci. Total Environ.*, **2010**,408, 23, 5972.
DOI: [10.1016/j.scitotenv.2010.08.048](https://doi.org/10.1016/j.scitotenv.2010.08.048)
8. B. Pare, P. Singh, S.B. Jonnalagadda, *Indian J. Chem., Sec A.*, **2009**, 48,1364.
[http://nopr.niscair.res.in/bitstream/123456789/6122/1/IJCA%2048A\(10\)%201364-1369.pdf](http://nopr.niscair.res.in/bitstream/123456789/6122/1/IJCA%2048A(10)%201364-1369.pdf)
9. S. Chakrabarti, B.K. Dutta, *J Hazard. Mater.*, **2004**, 112,3, 269.
DOI: [10.1016/j.jhazmat.2004.05.013](https://doi.org/10.1016/j.jhazmat.2004.05.013)
10. M. Shang, W. Wang, L. Zhang, *J. Hazard Mater.*, **2009**, 167,1 803.
DOI: [10.1016/j.jhazmat.2009.01.053](https://doi.org/10.1016/j.jhazmat.2009.01.053)
11. Xiaofeng Chang, Jun Huang, Shubo Deng, Gang Yu, *Catalysis Communications.*,**2010**, 11, 460.
DOI: [10.1016/j.catcom.2009.11.023](https://doi.org/10.1016/j.catcom.2009.11.023)
12. L. Zhang, W. Wang, L. Zhou, M. Shang, S. Sun, *Appl. Catal. B.*, **2009**, 90, 3, 458.
DOI: [10.1016/j.apcatb.2009.04.005](https://doi.org/10.1016/j.apcatb.2009.04.005)
13. D. Robert, S. Parra, C. Pulgarin, A. Hrzton, J. V. Weber, *Appl. Surf. Sci.*, **2000**,167, 51.
DOI: [Pii: S0169-4332\(00\)00496-7](https://doi.org/10.1016/S0169-4332(00)00496-7)
14. S. Qourzal, M. Tamimi, A. Assabbane, Y. Ait-Ichou, *J. Colloid. Interface Sci.*, **2005**, 286, 621.
DOI: [10.1016/j.jcis.2005.01.046](https://doi.org/10.1016/j.jcis.2005.01.046)
15. P. Singh, P. Raizada, S. Kumari, A. Kumar, D. Pathaniaa, P. Thakur, *Appl. Catal. A.*, **2014**, 476 , 9.
DOI: [10.1016/j.apcata.2014.02.009](https://doi.org/10.1016/j.apcata.2014.02.009)
16. T. Kawai, C. Ohtsuki, M. Kamitakahara, M. Tanihara, T. Miyazaki, Y. Sakaguchi, S. Konagaya, *Sci. Technol.*, **2006**, 40,13, 4281.
DOI: [10.1021/es050098n](https://doi.org/10.1021/es050098n)
17. Y. Komazaki, H. Shimizu, S. Tanaka, *Environ.*, **1999**, 33,27, 4363.
DOI: [http://dx.doi.org/10.1016/S1352-2310\(99\)00231-9](https://doi.org/10.1016/S1352-2310(99)00231-9)
18. W. Wei, R. Sun, J. Cui, Z. Wei, *Desalination.*, **2010**, 263,1, 89.
DOI: [10.1016/j.desal.2010.06.043](https://doi.org/10.1016/j.desal.2010.06.043)
19. E. Neyens, J. Baeyens, *J. Hazard. Mater.*, **2003**, 98, 3.
DOI: [10.1016/S0304-3894\(02\)00282-0](https://doi.org/10.1016/S0304-3894(02)00282-0)
20. B. Pare, P. Singh, S.B. Jonnalagadda, *J. Sci. Indus. Res.*, **2009**, 68,724.
[http://nopr.niscair.res.in/bitstream/123456789/5300/1/JSIR%2068\(8\)%20724-729.pdf](http://nopr.niscair.res.in/bitstream/123456789/5300/1/JSIR%2068(8)%20724-729.pdf)
21. P. Hui, S.L. Meena, G. Singh, R.D. Agarawal, S. Prakash, *J. Miner. Mater. Character. Eng.*, **2010**,92,683.
DOI: [file:///C:/Users/Dell_PC/Downloads/JMMCE2010080002_10652529.pdf](https://doi.org/10.1016/j.jmmce.2010.08.002)
22. E.M. Rivera, M. Araiza, W. Brostow , V. M. Castano, J.R. Diaz-Estrada, R. ernandez and J. R. Rodriguez, *Mater. Lett.*, **1999**,41, 128.
DOI: [Pii: S0167-577X\(99\)00118-4](https://doi.org/10.1016/S0167-577X(99)00118-4)
23. B. Pare, B. Sarwan S.B. Jonnalagadda, *J Mol. Struct.*, **2012**, 1007, 196.
DOI: [10.1016/j.molstruc.2011.10.046](https://doi.org/10.1016/j.molstruc.2011.10.046)
24. H. Eslami, M. Solati-Hashjin, M. Tahri, Iran. *J. Pharma. Sci.*, **2008**, 4,127.
DOI: [http://ijps.sums.ac.ir/files/PDFfiles/4th.pdf2066245936.pdf](https://doi.org/10.1016/j.jps.2008.02.011)
25. B. Cengiz Y. Gokce N. Yildiz, Z. Aktas, A. Calimli, *Collod. Surf. A.*, **2008**, 322, 29.
DOI: [10.1016/j.colsurfa.2008.02.011](https://doi.org/10.1016/j.colsurfa.2008.02.011)
26. S. Koutsopoulos, *J. Biomed. Mater. Res.*, **2002**,62,4,600.
DOI: [10.1002/jbm.10280](https://doi.org/10.1002/jbm.10280)
27. Q. Wang, J. Hui, Y. Huang, Y. Ding, Y. Cai, S. Yin, B. Su, *Mater. Sci. Semicond. Process*, **2014**, 17, 87.
DOI: [10.1016/j.mssp.2013.08.018](https://doi.org/10.1016/j.mssp.2013.08.018)
28. P. Raizada, P. Singh, A. Kumar, G. Sharma, B. Pare, S.B. Jonnalagadda, P.Thakur, *Appl. Catal. A.*, **2014**, 486, 159.
DOI: [10.1016/j.apcata.2014.08.043](https://doi.org/10.1016/j.apcata.2014.08.043)
29. B. Pare, P. Singh, S.B. Jonnalagadda, *Indian J. Chem. Technol.*, **2010**,17, 391.
DOI: [http://nopr.niscair.res.in/bitstream/123456789/6122/1/IJCA%2048A\(10\)%201364-1369.pdf](http://nopr.niscair.res.in/bitstream/123456789/6122/1/IJCA%2048A(10)%201364-1369.pdf)
30. P. Raizada, P. Singh, A. Kumar, B. Pare, S.B. Jonnalagadda, *Sep. Purif. Technol.*, **2014**,133,429.
DOI: [10.1016/j.seppur.2014.07.012](https://doi.org/10.1016/j.seppur.2014.07.012)
31. P. Kulshrestha, R.F. Giese, D.S. Aga, *Environ. Sci. Technol.* **2004**, 38, 4097.
DOI: [10.1021/es034856g](https://doi.org/10.1021/es034856g)
32. C. Zhaoa, M. Pelaezb, H. Deng, D. D. Dionysioub, *Appl. Catal. B: Environmental .*, **2013**, 134, 135, 83.
DOI: [10.1016/j.apcatb.2013.01.003](https://doi.org/10.1016/j.apcatb.2013.01.003)
33. G.V. Buxton, C. Greenstock, W.P. Hellman, A.B. Ross, *J. Phys. Chem. Ref. Data.*, **1988**, 17,513.
DOI: www3.nd.edu/~ndrlrcdc/Compilations/rxn.pdf
34. P. Singh, P. Raizada, D. Pathania, A. Kumar, P. Thakur, *Int. J. Photoenergy.*, **2013**,7, 7.
DOI: [10.1155/2013/726250](https://doi.org/10.1155/2013/726250)
35. H. Zhao, S. Xu, J. Zhong, X. Bao, *Catal. Today*, **2004**, 93, 857.
DOI: [10.1016/j.cattod.2004.06.086](https://doi.org/10.1016/j.cattod.2004.06.086)
36. B. Pare, P. Singh, S.B. Jonnalagadda, *Indian J. Chem. Sect. A.*, **2009**, 48, 1364.
DOI: [http://nopr.niscair.res.in/bitstream/123456789/6122/1/IJCA%2048A\(10\)%201364-1369.pdf](http://nopr.niscair.res.in/bitstream/123456789/6122/1/IJCA%2048A(10)%201364-1369.pdf)

Advanced Materials Letters

Copyright © 2016 VBRI Press AB, Sweden
www.vbripress.com/aml

Publish your article in this journal

Advanced Materials Letters is an official international journal of International Association of Advanced Materials (IAAM, www.iaamonline.org) published monthly by VBRI Press AB from Sweden. The journal is intended to provide high-quality peer-review articles in the fascinating field of materials science and technology particularly in the area of structure, synthesis and processing, characterisation, advanced-state properties and applications of materials. All published articles are indexed in various databases and are available download for free. The manuscript management system is completely electronic and has fast and fair peer-review process. The journal includes review article, research article, notes, letter to editor and short communications.



A Monthly Journal

